Structure factor of polymers interacting via a short range repulsive potential: Application to hairy wormlike micelles

Gladys Massiera,* Laurence Ramos, and Christian Ligoure
Groupe de Dynamique des Phases Condensées (CNRS-UM2 No. 5581), CC26, Université Montpellier 2, 34095 Montpellier Cedex 5, France

Estelle Pitard
Laboratoire de Physique Mathématique et Théorique (CNRS-UM2 No. 5825), CC50, Université Montpellier 2, 34095 Montpellier Cedex 5, France

(Received 9 January 2003; published 15 August 2003)

We use the random phase approximation to compute the structure factor $S(q)$ of a solution of chains interacting through a soft and short range repulsive potential V. Above a threshold polymer concentration, whose magnitude is essentially controlled by the range of the potential, $S(q)$ exhibits a peak whose position depends on the concentration. We take advantage of the close analogy between polymers and wormlike micelles and apply our model, using a Gaussian function for V, to quantitatively analyze experimental small angle neutron scattering profiles of solutions of hairy wormlike micelles. These samples, which consist in surfactant self-assembled flexible cylinders decorated by amphiphilic copolymer, provide indeed an appropriate experimental model system to study the structure of sterically interacting polymer solutions.

DOI: 10.1103/PhysRevE.68.021803 PACS number(s): 61.25.Hq, 83.80.Qr, 61.12.−q, 05.20.−y

I. INTRODUCTION

Isotropic solutions of unidimensional objects such as polymers do not generally show a correlation peak in their structure factor except for very concentrated systems and melts, or charged systems. For polyelectrolytes, the peak originates from strong electrostatic interchain interactions, whereas for neutral polymers the peak is observed at very large scattering vector, on the order of the inverse of the monomer length, and is the signature of a liquidlike order at the monomer length scale, as in simple liquids. Recently we have reported on one type of living polymer system, which also exhibits a structural peak in the scattering function, but with a totally different physical origin [1]. The experimental system is a solution of hairy wormlike micelles, obtained by adding small amounts of amphiphilic copolymer to a solution of surfactant micelles. The correlation peak, observed both at low concentration of micelles (semidilute regime) and at higher concentration (concentrated regime), originates from steric repulsion between the micelles, induced by the copolymer layer that covers them. Although the interaction is short range, with a range of the order of the copolymer layer thickness, it is sufficient to generate a correlation peak, as demonstrated by small angle neutron scattering (SANS) experiments. Because surfactant self-assemblies scatter light and neutron much stronger than polymers, surfactant wormlike micelles have appeared as a convenient model system for the study of the structure of polymer solutions [2]. In particular, charged wormlike micelles have been extensively studied as an alternative system to conventional polyelectrolyte solutions [3–5]. Similarly, hairy wormlike micelles may be a suitable model system to investigate steric interactions in solutions of polymers.

The random phase approximation (RPA) represents a powerful theoretical tool to predict the structure factor of polymeric systems, provided concentration fluctuations are weak. Introduced a long time ago in the context of simple liquids [6,7], it has been reformulated explicitly by Edwards in the framework of polymer theory [8], and has been applied since to numerous polymer systems, for instance, to polyelectrolytes solutions [9–12] or to microphase separation in block copolymers melts [13]. For concentrated polymer solutions, concentration fluctuations are weak, allowing a perturbative approach for the calculation of correlation functions, starting from the mean field Hamiltonian of the system. A perturbative calculation around the homogeneous equilibrium values of the monomer densities allows, in particular, the computation of the structure factor. In this paper, we add a Gaussian repulsive potential to the classical excluded volume interactions between monomers, using a RPA description of polymer solutions (using Edward's formalism) and calculate the structure factor $S(q)$. We show that $S(q)$ may exhibit a broad correlation peak, whose existence and position as a function of polymer concentration, range, and magnitude of the Gaussian potential are discussed. The behavior of the theoretical $S(q)$ appears in excellent qualitative concordance with the experimental SANS scattering profiles of hairy wormlike micelles. Moreover, we use our model to fit the experimental peak position as a function of the micellar concentration and derive a measurement of the thickness h of the polymer layer covering the micelle. The numerical values of h are found in good agreement with simple theoretical expectations and with other experimental determinations [14].

The paper is organized as follows. Section II describes the experimental system and recalls the main experimental results reported in Ref. [1] concerning the scattering patterns of semidilute solutions of hairy wormlike micelles. In Sec. III,

*Present address: Chemical and Biomolecular Engineering Department, University of Pennsylvania, Towne 311A, Philadelphia, Pennsylvania 19104, USA.

we describe a model based on the RPA technique, which allows one to predict the structure factor of polymer solutions that interact via a short-range repulsive potential. We comment on the validity of the RPA in the framework of semidilute and concentrated solutions of wormlike micelles and then apply the model to our specific experimental system. In Sec. IV we compare the model to the experiments and derive a quantitative evaluation for the thickness of the polymeric layer. We conclude in Sec. V. Technical details of the calculation are given in the Appendix.

II. EXPERIMENTS

A. Experimental system

Hairy polymers are obtained by adding to solutions of wormlike micelles small amounts of amphiphilic copolymer, whose hydrophobic part adsorbs onto the fluid surfactant cylinders and whose hydrophilic tail remains swollen in water and decorates the micelles. The surfactant micelles are formed by diluting in brine ($[\mathrm{NaCl}]=0.5\ M$) a mixture of cetylpyridinium chloride (CpCl) and sodium salicylate (NaSal) at a fixed molar ratio $[\mathrm{NaSal}]/[\mathrm{CpCl}]=0.5$ [15]. We use commercially available triblock copolymers (Synperonic F108 and F68, by Serva, used as received) and a diblock copolymer (PC18, synthesized in our laboratory [16]). The Synperonic F108 (F68) consists in two identical hydrophilic polyoxyethylene (POE) blocks of 127 (76) monomers each, symmetrically bounded to a central shorter hydrophobic block of polyoxypropylene (PPO) of 48 (29) monomers. The polymer PC18 consists in a C_{18} alkyl chain as hydrophobic part, bounded by an uretane group to a POE block of 113 monomers. The radii of gyration of the hydrophilic blocks are 18.6, 25.8, and 24 Å for F68, F108, and PC18, respectively. We have shown in Ref. [1] that the cylindrical structure of the micelles is maintained upon copolymer addition, with a constant radius of their hydrophobic core $r_C \approx 21$ Å. We define ϕ as the surfactant volume fraction and α as the PEO-block to surfactant molar ratio. In our experiments, we vary ϕ and α between 2.8 and 40% and 0 and 4.2%, respectively. The parameter α controls the density of the polymeric layer. The crossover α^* between the mushroom regime and the brush regime [17] being estimated to 3%, 1.5%, and 1.8% for F68, F108, and PC18, respectively, both regimes are probed in our experiments. On the other hand, the surfactant concentrations investigated are all above the critical overlap concentration that separates the dilute regime to the semidilute regime.

SANS experiments are performed on the spectrometer PACE at the Laboratoire Léon Brillouin (Saclay, France) and on the D11 beam line at the Institut Laue Langevin (Grenoble, France). We use deuterated water, all other components being hydrogenated. Neutron experiments are thus sensitive to the contrast between the hydrophobic core of the micelles and the aqueous solvent (D_20). In particular, because the hydrophilic POE blocks of the copolymer are always highly swollen in D_20, the contribution of the copolymer layer to the scattered intensity is negligible compared to the contribution of the hydrophobic core and thus the copolymer layer covering the micelles is not directly probed. Temperature is fixed at 30°C.

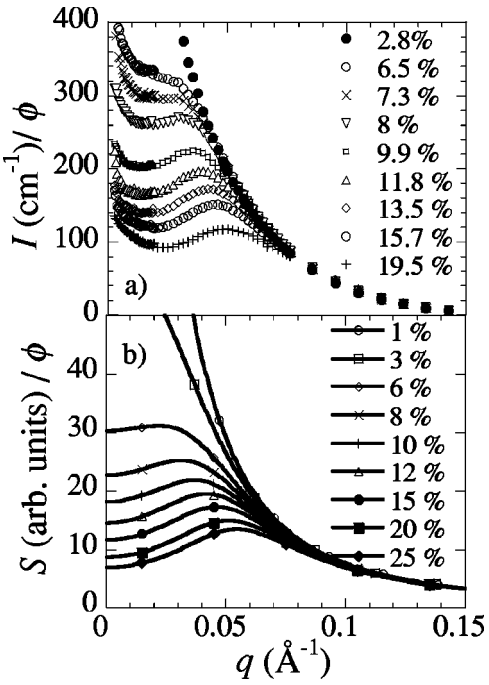

FIG. 1. (a) Experimental scattering profiles and (b) theoretical structure factors, normalized by surfactant volume fraction ϕ. Curves are labeled by surfactant volume fraction ϕ. In (a), the copolymer (F108) over surfactant ratio is $\alpha=1\%$; in (b), the amplitude and range of the Gaussian potential are $U_0=800k_BT$ and $\delta=34$ Å, respectively.

B. Correlation peak

In this section, we recall the main experimental results previously reported by us in Ref. [1]. Figure 1(a) shows the variation of the scattering profile for samples with constant copolymer density ($\alpha=1\%$) but with various surfactant volume fractions ϕ. The scattering profile is monotonically decreasing at low ϕ and above a threshold surfactant volume fraction ϕ_c, a correlation peak is observed at a finite wave vector. The intensity of the peak increases with ϕ and its position q^* is reported to higher wave vector when ϕ increases. Figure 2(a) shows the variation of the scattering profile at a fixed surfactant volume fraction $\phi=9\%$ when the copolymer density is increased. A peak emerges above a threshold copolymer molar ratio and becomes more and more pronounced and narrow as α increases. Moreover, the peak position varies only weakly with the copolymer to surfactant ratio. We note that these features are obtained for the three types of copolymer used.

Because of the high ionic strength ($0.5\ M$), electrostatic interactions are screened and are thus not relevant in our experiments. The correlation peak observed experimentally, whose intensity increases with the copolymer over surfactant ratio, originates therefore from the copolymer layer adsorbed onto the micelles. This layer creates a steric short-range repulsion between the micelles, with a range on the order of the copolymer layer thickness. To analyze more quantita-

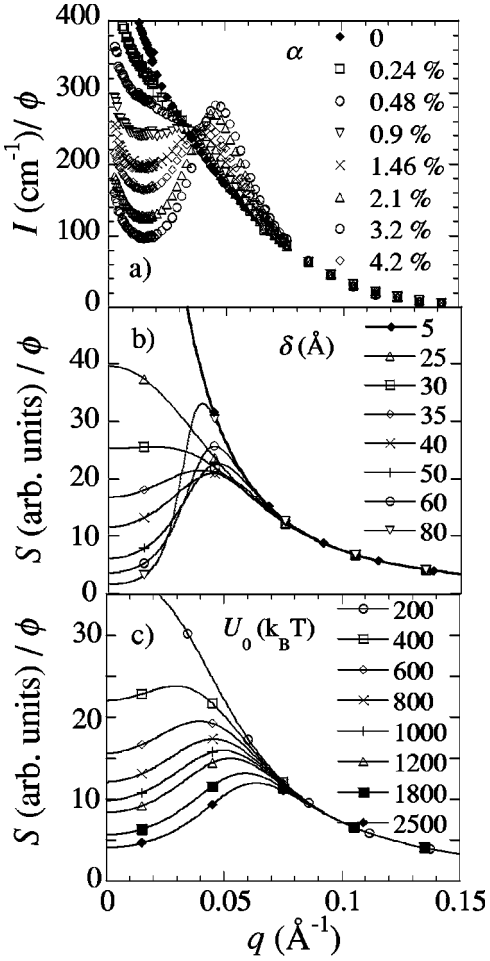

FIG. 2. (a) Experimental scattering profiles and (b,c) theoretical structure factors, normalized by surfactant volume fraction ϕ. In (a), the surfactant volume fraction is $\phi=9\%$ and curves are labeled by copolymer (F108) over surfactant ratio α. In (b) and (c), the surfactant volume fraction is $\phi=10\%$. In (b) the amplitude of the potential is $U_0=800k_BT$ and curves are labeled by the range of the potential δ. In (c), the range of the potential is $\delta=34$ Å and curves are labeled by the amplitude of the potential U_0.

tively the scattering profiles, we model the soft short-range copolymer-induced repulsion and use the RPA technique to compute the structure factor of a solution of polymeric chains interacting via a short-range repulsion.

III. THEORETICAL ANALYSIS

A. RPA Model

In a continuous approach, the Hamiltonian $\mathcal{H}(\vec{r}(s))$ of a linear chain of N statistical units in a given configuration $\vec{r}(s)$ reads, in k_BT units,

$$\mathcal{H}(\vec{r}(s))=\frac{3}{2a^2}\int_0^N ds\left(\frac{\partial\vec{r}}{\partial s}\right)^2 + \frac{1}{2}\int_0^N\int_0^N ds\,ds'\,\mathbf{V}(\vec{r}(s)-\vec{r}(s')), \qquad (1)$$

where a is the monomer size, $\vec{r}(s)$ is the position of the sth monomer, and $\mathbf{V}(\vec{r}-\vec{r'})$ is the monomer-monomer interaction potential. The first term of the right-hand side of Eq. (1) represents the entropic contribution of the chain configurations (the ''entropic elasticity'') and the second term describes the two-body interaction. From this Hamiltonian, we calculate the partition function of the system, and we evaluate the monomer density autocorrelation function, which is directly proportional to the structure factor $S(q)$. The details of these calculations are given in the Appendix and can be generalized to a system of M independent chains containing each N monomers [18]. The result is a classical general expression for the structure factor for any given microscopic potential $\mathbf{V}(\vec{r})$ between monomers:

$$S^{-1}(\vec{q})=S_0^{-1}(\vec{q})+\tilde{\mathbf{V}}(\vec{q}), \qquad (2)$$

where $\tilde{\mathbf{V}}(\vec{q})$ is the Fourier transform of $\mathbf{V}(\vec{r})$ and $S_0(\vec{q})$ is the structure factor of a Gaussian chain without interaction:

$$S_0(\vec{q})=NV\rho_0 f((qR_G)^2). \qquad (3)$$

In Eq. (3), N is the number of monomers per chain, R_G is the radius of gyration of one chain, V is the total volume, ρ_0 is the homogeneous equilibrium density of monomers, and $f(x)=2/x^2(e^{-x}+x-1)$ is the Debye function.

Hence, Eq. (2) allows one to calculate the structure factor of semidilute solutions of polymers for any given interaction potential between monomers. This equation can be used for hairy wormlike micelles, once a phenomenological potential $\mathbf{V}(\vec{r})$ is given to account for the steric repulsion.

B. Phenomenological repulsive potential

We assume that the interaction potential between hairy polymers can be considered as the sum of a standard excluded volume potential (polymer-solvent interactions) $v_0\delta(\vec{r})$ and an additional repulsive potential $V_g(\vec{r})$, due to the steric layer. The two physical criteria for this steric potential are that $V_g(\vec{r})$ should be soft and short range. We thus choose to model it with a Gaussian function, which decreases sufficiently fast to be considered as short range:

$$V_g(\vec{r})=U_0\exp\left(-\frac{r^2}{2\delta^2}\right). \qquad (4)$$

We expect δ, the width of the Gaussian, to be on the order of the steric layer thickness. We moreover expect both δ and the amplitude of the repulsive potential U_0 to increase as the amount of copolymer α increases. We note that a Gaussian form for the potential has been recently justified for some soft interacting objects, such as polymer coils [19,20], flexible dendrimers [21], or star polymers near the θ point [22]. A Gaussian shape has the advantage of leading to a simple analytical expression for the structure factor of hairy polymers:

$$VS^{-1}(\vec{q}) = VS_0^{-1}(\vec{q}) + v_0 + U_0(2\pi\delta^2)^{3/2}\exp\left(-\frac{(q\delta)^2}{2}\right). \quad (5)$$

The last two terms of the right-hand side of Eq. (5) represent the interaction part of the structure factor: v_0 is the excluded volume parameter and the last term is the Fourier transform of $V_g(\vec{r})$.

C. Theoretical structure factor and comparison with experiments

Because RPA essentially neglects strong density fluctuations (see Appendix and Refs. [18,23]), this approximation is *a priori* best suited for concentrated solutions or melts of polymer. However, RPA can nevertheless be applied to less concentrated solutions, provided fluctuations are weak [18]. In particular, in Ref. [24], the validity of RPA for semidilute solutions is discussed. The authors show that a renormalization of the excluded volume parameter leads to a very good agreement between the RPA and the renormalization group theory. For giant micelles, a concentrated regime is reached even at relatively low surfactant concentration, $\phi \approx 0.1$, because of the large persistence length of the micelles, as demonstrated by both experiments and simulations [25,26]. A concentrated regime is indeed attained as soon as the correlation length ξ is on the order of l_P, which eventually occurs in the range of concentration investigated experimentally (ϕ in the range 0.028–0.4). Note, however, that in the same range of concentration both rheology [27] and light scattering [28] experiments indicate that ξ varies as $\phi^{-3/4}$, a scaling characteristic of a semidilute solution, in seeming contradiction with the system being in a concentrated regime. This apparent discrepancy underlines how the border between semidilute and concentrated solutions is ill defined for wormlike micelles solutions.

Given these restrictions, we can now apply the RPA results to semidilute and concentrated solutions of wormlike micelles. Hence, we use Eq. (5) to compute the structure factor of solutions of hairy micelles and investigate their variation with the micellar concentration and characteristics of the copolymer-induced Gaussian potential. We define the statistical unit or ''monomer'' as a slice of micelle of length a equal to $2\,l_P$, where $l_P \simeq 190$ Å is the persistence length of the micelle, and of radius $r_0 \simeq 30$ Å [29,30]. The equilibrium density of monomers, ρ_0, is then related to the surfactant volume fraction by $\rho_0 = \phi/2\pi r_0^2 l_P$. The number of statistical units per chain obeys [31]

$$N = \frac{a_0^2}{4\pi r_0 l_P}\left(\frac{v_{sol.}}{v_{t.a.}}\right)^{-1/2}\phi^{1/2}\exp[E/2k_BT],$$

where $a_0 = 7.2$ Å is the surfactant polar head diameter, $E \approx 26\,k_BT$ is the end-cap energy, and $v_{sol.} \approx 30$ Å^3 and $v_{t.a.} \approx 595$ Å^3 are the volume of a molecule of solvent and of surfactant, respectively. The expression for N is then used to calculate the radius of gyration of a chain: $R_G = a\sqrt{N}/\sqrt{6}$. The excluded parameter is fixed to $v_0 = a^3$, which corresponds to a polymer in an athermal solvent.

With excluded volume as unique interaction potential, Eq. (5) is reduced to the classical expression first derived by Edwards [18] for a polymer chain with excluded volume interactions and the structure factor is a monotonically decreasing function of the q vector. By contrast, in the presence of a Gaussian potential, we show that the structure factor $S(q)$ may have a nonmonotonic variation and may exhibit a peak at a finite wave vector q^*. The condition for the existence of a peak can be determined from the analytical expression of the structure factor [Eq. (5)]. This is easily calculated if we note that the derivative of the inverse of the Debye function $f^{-1}(x)$ tends to 1/2 for large x, while it tends to 1/3 when x is small. Assuming that $(qR_G)^2 \gg 1$, which is always verified in the neighborhood of the peak, we obtain that the structure factor displays a peak for surfactant volume fraction ϕ larger than a threshold value ϕ_c:

$$\phi_c = \frac{4\pi r_0^2 l_P^3}{3(2\pi)^{3/2}}\frac{1}{\delta^5 U_0}, \quad (6)$$

and the position q^* of the peak is given by

$$q^* = \frac{\sqrt{2}}{\delta}\sqrt{\ln\left(\frac{\phi}{\phi_c}\right)} = \frac{\sqrt{2}}{\delta}\sqrt{\ln\left(\frac{3(2\pi)^{3/2}}{4\pi r_0^2 l_P^3}\phi\delta^5 U_0\right)}. \quad (7)$$

The critical volume fraction depends on the two parameters characterizing the Gaussian potential, δ and U_0. It decreases as either the range or the amplitude of the potential increases, but ϕ_c is more sensitive to δ than to U_0. Note that the peak position is independent of the excluded volume parameter v_0; in fact, ϕ_c diverges if the unique repulsive potential is the excluded volume ($\delta = 0$ or $U_0 = 0$), consistently with the structure factor being strictly decreasing, as mentioned above.

In order to directly compare the theoretical structure factors with experiments, we first choose fixed values for the parameters of the Gaussian potential, which should correspond to keeping the copolymer over surfactant molar ratio α constant, and we vary the surfactant volume fraction. The theoretical structure factors obtained for $\delta = 34$ Å and $U_0 = 800\,k_BT$ are plotted in Fig. 1(b) and exhibit features very similar to the experimental scattering profiles [Fig. 1(a)]. At low ϕ, the structure factor is a decreasing function of the wave vector. By contrast, for $\phi \simeq 6\%$, a correlation peak appears, which becomes more and more narrow and whose position is reported to higher wave vector as ϕ increases. On the other hand, when the copolymer over surfactant molar ratio α is experimentally varied, the copolymer-induced steric potential changes and thus the two characteristic parameters of the Gaussian potential should change as well. However, there is no clear intuitive argument how to determine the influence of α on δ and U_0 separately. To mimic experimental data taken at various α, we therefore vary independently δ and U_0. The structure factors obtained for $\phi = 10\%$, $U_0 = 800\,k_BT$ and δ in the range 5–80 Å are plotted

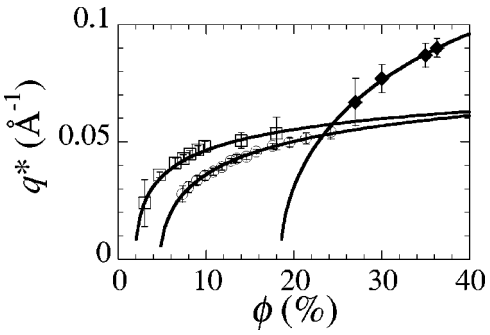

FIG. 3. Variation of the peak position with surfactant volume fraction for samples without copolymer (diamonds) and with a copolymer (F108) over surfactant ratio $\alpha=1\%$ (empty circles) and $\alpha=3.2\%$ (empty squares). Symbols are experimental data points and lines are best fits, using Eq. (7). The fitting parameters are given in Table I.

in Fig. 2(b), while the structure factors obtained for $\phi=10\%$, $\delta=30$ Å and U_0 in the range 200–2500 k_BT are plotted in Fig. 2(c). Both series display features very similar to the experimental scattering profiles shown in Fig. 2(a). For a fixed amplitude U_0 of the potential, a correlation peak appears for δ larger than 30 Å and becomes more pronounced as δ increases. Similarly, increasing U_0 with fixed δ leads to the emergence of a peak and to an increase of its intensity. In the two cases, similar to what is obtained experimentally upon increasing α, the parameters δ and U_0 have poor influence on the peak position.

Thus, the theoretical structure factors capture the essential features of the experimental scattering profiles and their evolution with the experimental parameters. However, the comparison between theory and experiment can only be qualitative, since theory describes the correlation between the objects and does not take into account the form of the scattering objects, whereas the scattered intensity is experimentally measured. While the relation between scattered intensity $I(q)$ and structure and form factors $S(q)$ and $P(q)$ is simple for spherical objects $[I(q)=P(q)S(q)]$, it is more complex for semidilute solutions of linear and flexible objects. Moreover, the RPA technique usually does not describe correctly the structure factor at very low q. These two limitations make it more difficult to fit precisely the experimental scattering profiles, though remarkable agreement with the experimental position of the peak can be found, as shown in the following section.

IV. DISCUSSION

A. Fit of the peak position

To analyze more quantitatively our data, we assume that the experimental peak position in the scattered intensity is correctly described by the theoretical structure factor. For surfactant volume fraction above the critical surfactant volume fraction ϕ_c, the peak position q^* is given by Eq. (7). We use this equation to fit the experimental ϕ dependence of q^*, with δ and U_0 as fitting parameters. As shown in Fig. 3, a very good fit is obtained for the experimental data obtained for hairy micelles decorated with different amounts of copolymer F108 as well as for naked micelles [34]. An equally good agreement is obtained for the two other copolymers (data not shown). The results of the fits are given in Table I for all experimental configurations.

In the case of naked micelles, a correlation peak is detected only at a very large concentration (ϕ above 24%) and the ϕ dependence of q^* can hence be fitted only in a reduced range of concentrations. We find for the fitting parameters $U_0=24604$ k_BT and $\delta=13$ Å, which correspond to a very high and narrow potential. For hairy micelles, the fits always extend over a larger interval of concentrations than that for naked micelles. The values of U_0 range between 790 and 2770 k_BT and those of δ range between 26 and 39 Å. Hence, the range of the potential is on the order of the radius of gyration of the copolymer, and is always larger than that of naked micelles. It, moreover, increases from 33.7 to 38.7 Å when α increases from 1% to 3.2% (for F108 copolymer). In addition, we find δ smaller for the copolymer F68 than for the copolymers PC18 or F108, as expected, since F68 possesses shorter hydrophilic chains than F108 or PC18. On the other hand, we find that, in the presence of the copolymer layer, the amplitude of the potential is considerably reduced compared to the case of naked micelles. This can be intuitively understood. Indeed, the copolymer layer covering the micelles is presumably very compressible, since this layer is highly swollen by the solvent (the regime of a dry brush is never reached experimentally, α being always comparable to the overlap threshold α^*). This should result in a small value for U_0, much smaller than for naked micelles for which the dense shell of surfactant polar heads is very little compressible. For naked micelles, a potential close to a hard core potential is expected, consistently with our results. Although the values of the amplitude U_0 that we extract from the fits may seem very high, they correspond to very reason-

TABLE I. Fitting parameters, range δ, and amplitude U_0 of the Gaussian potential, effective thickness of the copolymer layer, h, and theoretical and experimental critical volume fraction above which a correlation peak appears, for samples with different copolymers and different amounts of copolymer.

	δ (Å)	U_0 (k_BT)	h (Å)	Theoretical ϕ_c	Experimental ϕ_c
$\alpha=0$	13	24604		18%	25.5 ± 1.5 %
F108, $\alpha=1\%$	33.7	793	31.6	4.8%	7.3 ± 0.7 %
F108, $\alpha=3.2\%$	38.7	1007	41.9	1.9%	3 ± 1 %
F68, $\alpha=2.1\%$	25.7	2768	21.2	5.3%	8 ± 1 %
PC18, $\alpha=2.1\%$	33.6	1196	33.2	3.2%	4.9 ± 1.9 %

able values for the mean free energy per anchored polymer tail of roughly $15k_BT$.

One could *a priori* separate the contribution of the surfactant shell from that of the copolymer layer, by replacing the Gaussian potential in Eq. (2) by the sum of two Gaussian functions, one accounting for the surfactant contribution and the other one for the copolymer contribution. The former Gaussian function is expected to be very narrow and high, reflecting an excluded volume interaction, while the latter is expected wider and lower. We can compute the structure factors in this approach, by taking for the former potential the parameters derived from the fit of the naked micelles and letting free the parameters (α^{copo} and U_0^{copo}) for the copolymer contribution. In this case, we find that the essential features of the theoretical structure factors and their evolution with ϕ, α^{copo} and U_0^{copo} remain unchanged. Moreover, the values of α^{copo} and U_0^{copo}, derived from the ϕ dependence of q^*, which should account solely for the copolymer layer, are of the same order of magnitude as the values obtained with one Gaussian function, although U_0^{copo} is slightly smaller than U_0. This strongly suggests that only the tail of the potential (of energy at most of a few k_BT) is relevant and that this tail does not vary much with the addition of a high and narrow potential. Moreover, it is clear that the concavity of the potential $V_g(\vec{r})$ is nonphysical for $r<\delta$, limiting the validity of a Gaussian potential to not too short distances.

Finally, we compare the theoretical values of ϕ_c, deduced from the fitting parameters using Eq. (6), to the experimental concentrations. As can be seen in Table I, the experimental values show the same variations as the theoretical ones but are systematically smaller. This discrepancy could originate from the fact that it is the scattered intensity I that is experimentally measured, while the structure factor is computed theoretically. Peaks of low magnitude in the structure factor may thus be masked in a I vs q plot because of the form factor of the objects, which is a decreasing function of the q vector.

B. Effective thickness of the copolymer layer

The pair of fitting parameters δ and U_0 allows a determination of an effective thickness of the copolymer layer, h. The simple physical criterion we apply is based on the assumption that the micelles enter in contact as soon as their interaction potential overcomes the thermal energy k_BT. Thus, for a monomer-monomer distance $r=2(r_0+h)$, the Gaussian potential is equal to $1k_BT$ and $V_g(r)=U_0\exp(-r^2/2\delta^2)=1$. This criterion leads to a relation between the effective thickness h, the naked radius of the micelles r_0, and the potential parameters δ and U_0:

$$r_0+h=\delta\sqrt{(\ln U_0)/2}. \tag{8}$$

Using this simple criterion for naked micelles, we obtain $r_0=29.2$ Å (h being equal to 0 by definition in this case), a value in striking good agreement with the expected value ($r_0\simeq 30$ Å [29,30]). The values of h deduced from the fitting parameters δ and U_0 are reported in Table I for hairy micelles and are very close to the radii of gyration of the copolymers. They are also very close, although slightly larger, to the values deduced from two other independent methods [14]. They, moreover, follow the expected trends: h increases with the amount of copolymer and is larger when the polymer is longer.

C. Microscopic model for the copolymer-induced repulsive potential

At this point of the discussion, one can finally raise the question of the microscopic origin of the Gaussian potential used here. With this function for the potential, the model describes correctly the behavior of the scattering profiles and especially the variation of the peak position with ϕ. It appears nevertheless difficult to draw a precise link between the microscopic details of the system and the effective mean-field potential. Qualitatively, one can, however, suggest the following physical picture: the Gaussian potential originates from the copolymer layer covering the wormlike micelles, inducing thereby an additional steric repulsion. Two regimes have to be considered. In the brush regime the micelles are covered with a semidilute copolymer layer, while in the mushroom regime the copolymer chains are isolated on the micelles. The interaction is clearly stronger and with a larger range in the brush regime. In order to bring two micelles close to each other, a large energy is needed to compensate the energy cost to compress the copolymer layer below its equilibrium thickness value. This compression energy leads to a strong repulsion that is relevant for short distances r between micelles. This energy can be evaluated from the gap in energy between the equilibrium brush free energy and its value at r in the brush regime, while in the mushroom regime the energy can be evaluated from the energy cost for confining the polymer on distances smaller than its Flory radius. Although the theoretical potentials calculated with this approach [32] cannot be satisfactorily fit with a Gaussian function, they give numerical values of h in excellent agreement with those deduced from the q^* vs ϕ fits.

V. CONCLUSION

To conclude, we have shown that a RPA approach starting from an Edwards Hamiltonian with a soft Gaussian repulsive potential reproduces qualitatively the experimental results obtained for the structure of hairy wormlike micelles. In particular, the correlation peak on the micellar concentration ϕ is in agreement with the theoretical variation. This model allows one to extract physical parameters with very reasonable numerical values.

The motivation of our study was to understand and reproduce in a simple way the existence of a peak at intermediate q vector in the structure factor and not to have a perfect description of the full $I(q)$ curve. Alternative, more refined, techniques exist. For instance, in Ref. [33], Pedersen and Schurtenberger show that a polymer reference interaction site model (PRISM) equation reproduces more accurately the full $I(q)$ curve for solutions of polystyrene than does a RPA equation with only δ excluded volume interactions. Note, however, that the PRISM equation in their paper can be interpreted as a RPA equation where the Fourier transform of the potential is now $c(q)$, hence formally modi-

fying the δ excluded volume potential by introducing the analog of a form factor. In our case we could also use a PRISM-like equation that would take into account the form factor of the objects in addition to the Gaussian potential introduced in Eq. (2). Analyzing the full experimental $I(q)$ curves with this approach could be very interesting, a severe drawback being, however, a less simple understanding of the physical origin of the peak in the structure factor.

Finally, we believe that hairy wormlike micelles solutions provide an original experimental system to illustrate the influence of a soft short range repulsion in isotropic solutions of linear flexible objects. The interaction induced by the copolymer layer is soft but sufficiently strong to induce a correlation peak in the structure factor. The random phase approximation has proven to be helpful in describing the qualitative behavior of the scattered patterns. Such a model may be used in a variety of ''hairy linear objects,'' such as copolymer micelles, or hairy polymers (comblike polymers), for which the interaction is short range.

ACKNOWLEDGMENTS

We are grateful to R. Aznar for the synthesis of the PC18. Local contacts, L. Auvray at LLB and B. Demé and J. Zipfel at ILL, are acknowledged. E.P. thanks Henri Orland for very useful discussions. We would like to thank an anonymous referee for useful comments and suggestions.

APPENDIX

In this appendix, we detail the structure factor calculation for the RPA.

From the Hamiltonian in k_BT units [Eq. (1)],

$$\mathcal{H}(\vec{r}(s))=\frac{3}{2a^2}\int_0^N ds\left(\frac{\partial\vec{r}}{\partial s}\right)^2 + \frac{1}{2}\int\int_0^N ds\,ds'\,\mathbf{V}(\vec{r}(s)-\vec{r}(s')), \quad \text{(A1)}$$

we can evaluate the chain partition function $\mathcal{Z}$ as the sum, over all the configurations $\vec{r}(s)$, of the Boltzmann factor:

$$\mathcal{Z}=\int D\vec{r}(s)\exp[-\mathcal{H}(\vec{r}(s))]. \quad \text{(A2)}$$

The local monomer density is defined as

$$\rho(\vec{r}(s))=\int_0^N ds\,\delta(\vec{r}-\vec{r}(s)). \quad \text{(A3)}$$

From the definition of $\rho(\vec{r}(s))$, we can write the identity

$$\int D\rho(\vec{r})\,\delta\left(\rho(\vec{r}(s))-\int_0^N ds\,\delta(\vec{r}-\vec{r}(s))\right)=1, \quad \text{(A4)}$$

which can also be expressed in the Fourier functional space

$$\int D\rho(\vec{r})\int D\hat{\rho}(\vec{r})\exp\left[i\int d\vec{r}\hat{\rho}(\vec{r})\rho(\vec{r})-i\int ds\,\hat{\rho}(\vec{r}(s))\right] = 1. \quad \text{(A5)}$$

By introducing this identity into the partition function, $\mathcal{Z}$ can be expressed as a function of collective variables $\rho(\vec{r})$ and $\hat{\rho}(\vec{r})$, the local density and its conjugate variable in the Fourier space:

$$\mathcal{Z}=\int D\rho(\vec{r})D\hat{\rho}(\vec{r})\exp[-\mathcal{F}(\{\rho(\vec{r}),\hat{\rho}(\vec{r})\})], \quad \text{(A6)}$$

with

$$\mathcal{F}(\{\rho(\vec{r}),\hat{\rho}(\vec{r})\})=-\ln[\zeta(\{i\hat{\rho}(\vec{r})\})]-i\int d\vec{r}\hat{\rho}(\vec{r})\rho(\vec{r}) + \frac{1}{2}\int d\vec{r}d\vec{r'}\rho(\vec{r})\mathbf{V}(\vec{r}-\vec{r'})\rho(\vec{r'}) \quad \text{(A7)}$$

and where $\zeta(\{i\hat{\rho}(\vec{r})\})$ is a function of $\hat{\rho}(\vec{r})$ only:

$$\zeta(\{i\hat{\rho}(\vec{r})\})=\int D\vec{r}(s)\exp\left[-\frac{3}{2a^2}\int ds\left(\frac{\partial\vec{r}(s)}{\partial s}\right)^2\right] \times\exp\left[-i\int d\vec{r}\hat{\rho}(\vec{r})\int ds\,\delta(\vec{r}-\vec{r}(s))\right]. \quad \text{(A8)}$$

By minimizing the free energy $\mathcal{F}(\{\rho(\vec{r}),\hat{\rho}(\vec{r})\})$ with respect to both $\rho(\vec{r})$ and $\hat{\rho}(\vec{r})$ we obtain ρ_0 and $\hat{\rho}_0$, the equilibrium homogeneous densities:

$$\left.\frac{\partial\mathcal{F}}{\partial\rho(\vec{r})}\right|_{\rho_0}=0 \quad \left.\frac{\partial\mathcal{F}}{\partial i\hat{\rho}(\vec{r})}\right|_{i\hat{\rho}_0}=0 \quad \Leftrightarrow \quad \rho_0=\frac{N}{V}, \quad i\hat{\rho}_0=\rho_0 W,$$

where $W=\int d\vec{r}\,\mathbf{V}(\vec{r})$ and V is the total volume.

Assuming fluctuations are weak, we develop a perturbative calculus around the equilibrium homogeneous densities $\{\rho_0,\hat{\rho}_0\}$:

$$\rho(\vec{r})=\rho_0+\delta\rho(\vec{r}),$$
$$\hat{\rho}(\vec{r})=\hat{\rho}_0+\delta\hat{\rho}(\vec{r}).$$

In $\mathcal{Z}$, we only keep constant terms (which contribute to the prefactor $\mathcal{Z}_0$) , and the terms of second order in $\{\delta\rho(\vec{r}),\delta\hat{\rho}(\vec{r})\}$, the sum of the first order terms being equal to 0. The partition function thus reads

$$\mathcal{Z}=\mathcal{Z}_0\int D\,\delta\rho(\vec{r})D\,\delta\hat{\rho}(\vec{r})\exp\left[i\int d\vec{r}\,\delta\rho(\vec{r})\,\delta\hat{\rho}(\vec{r})\right] \times\exp\left[-\frac{1}{2}\int d\vec{r}d\vec{r'}\,\delta\rho(\vec{r})\mathbf{V}(\vec{r}-\vec{r'})\,\delta\rho(\vec{r'})\right] \times\exp\left[-\frac{1}{2}\int d\vec{r}d\vec{r'}\,\delta\hat{\rho}(\vec{r})\frac{\rho_0}{V}g_D(\vec{r}-\vec{r'})\,\delta\hat{\rho}(\vec{r'})\right]. \quad \text{(A9)}$$

The function $g_D(\vec{r}-\vec{r'})$ is the correlation function of a Gaussian chain:

$$g_D(\vec{r}-\vec{r'})=\frac{V^2}{N}\int D\vec{r}(s)\exp\left[-\frac{3}{2a^2}\int ds\left(\frac{\partial\vec{r}(s)}{\partial s}\right)^2\right]\times\int ds\,\delta(\vec{r}-\vec{r}(s))\int ds'\,\delta(\vec{r'}-\vec{r}(s')). \tag{A10}$$

Finally, in the Fourier space, the partition function reads

$$\mathcal{Z}=\mathcal{Z}_0\int D\,\delta\rho(\vec{q})D\,\delta\hat{\rho}(\vec{q})\exp\left[-\frac{1}{2}\int d\vec{q}(\delta\rho(\vec{q}),\delta\hat{\rho}(\vec{q}))A\times(\vec{q})\begin{pmatrix}\delta\rho(-\vec{q})\\ \delta\hat{\rho}(-\vec{q})\end{pmatrix}\right],$$

where the matrix $A(\vec{q})$ is equal to

$$A(\vec{q})=V^2\begin{pmatrix}V\tilde{\mathbf{V}}(\vec{q}) & -i\\ -i & \rho_0 g_D(\vec{q}),\end{pmatrix},$$

where $\tilde{\mathbf{V}}(\vec{q})$ is the Fourier transform of the interaction potential:

$$\tilde{\mathbf{V}}(\vec{q})=\frac{1}{V}\int d\vec{r}\,e^{-\vec{q}\cdot\vec{r}}\mathbf{V}(\vec{r}). \tag{A11}$$

Finally, the Fourier transform of the density fluctuation correlation, which is proportionnal to the structure factor, reads

$$S(\vec{q})=V^2\langle\delta\rho(\vec{q})\,\delta\rho(-\vec{q})\rangle=V^3[A^{-1}(\vec{q})]_{11}. \tag{A12}$$

We thus obtain the simple form of Eq. (2) for the structure factor $S(\vec{q})$:

$$S^{-1}(\vec{q})=S_0^{-1}(\vec{q})+\tilde{\mathbf{V}}(\vec{q}), \tag{A13}$$

where $S_0(\vec{q})=N\rho_0 Vf((qR_G)^2)$, and $f(x)=2/x^2(e^{-x}+x-1)$ is the Debye function.

[1] G. Massiera, L. Ramos, and C. Ligoure, Langmuir **18**, 5687 (2002).
[2] L.M. Walker, Curr. Opin. Colloid Interface Sci. **6**, 451 (2001).
[3] L.J. Magid, J. Phys. Chem. B **102**, 4064 (1998).
[4] V. Schmitt and F. Lequeux, J. Phys. II **5**, 193 (1995).
[5] L. Cannavacciuolo, J.S. Pedersen, and P. Schurtenberger, Langmuir **18**, 2922 (2002).
[6] H.C. Andersen and D. Chandler, J. Chem. Phys. **53**, 547 (1970).
[7] J.-P. Hansen and I. R. McDonald, *Theory of Simple Liquids* (Academic Press, London, 1990).
[8] S.F. Edwards, Proc. Phys. Soc. London **88**, 265 (1966).
[9] J.-L. Barrat and J.-F. Joanny, Adv. Chem. Phys. **XCICV**, 1 (1996).
[10] V.Y. Borue and I.Y. Erukhimovich, Macromolecules **21**, 3240 (1988).
[11] J.-F. Joanny and L. Leibler, J. Phys. (France) **51**, 545 (1990).
[12] M. Castelnovo and J.-F. Joanny, Eur. Phys. J. E **6**, 377 (2001).
[13] L. Leibler, Macromolecules **13**, 1602 (1980).
[14] G. Massiera, L. Ramos, E. Pitard, and C. Ligoure, J. Phys.: Condens. Matter **15**, S225 (2003).
[15] H. Rehage and H. Hoffmann, J. Phys. Chem. **92**, 4712 (1988).
[16] P. Hartmann, M. Viguier, A. Collet, and D. Calvet, J. Fluorine Chem. **95**, 145 (1999).
[17] P.-G. De Gennes, Macromolecules **13**, 1069 (1980).
[18] M. Doi and S. F. Edwards, *The Theory of Polymer Dynamics*, International Series of Monographs on Physics Vol. 73 (Clarendon Press, Oxford, 1986).
[19] A.A. Louis, P.G. Bolhuis, J.-P. Hansen, and E.J. Meijer, Phys. Rev. Lett. **85**, 2522 (2000).
[20] P.G. Bolhuis, A.A. Louis, J.-P. Hansen, and E.J. Meijer, J. Chem. Phys. **114**, 4296 (2001).
[21] C.N. Likos, S. Rosenfeldt, N. Dingeouts, M. Ballauff, P. Lindner, N. Werner, and F. Vogtle, J. Chem. Phys. **117**, 1869 (2002).
[22] H. Graf and H. Löween, Phys. Rev. E **57**, 5744 (1998).
[23] P.-G. De Gennes, *Scaling Concepts in Polymer Physics* (Cornell University, New York, 1979).
[24] M. Müller, K. Binder, and L. Schäfer, Macromolecules **33**, 4568 (2000).
[25] A. Milchev, J.P. Wittmer, P. Van der Schoot, and D. Landau, Europhys. Lett. **54**, 58 (2001).
[26] E. Buhler, J.-P. Munch, and S.J. Candau, J. Phys. II **5**, 765 (1995).
[27] G. Massiera, L. Ramos, and C. Ligoure, Europhys. Lett. **57**, 127 (2002).
[28] J.-F. Berret, J. Appell, and G. Porte, Langmuir **9**, 2851 (1993).
[29] J. Marignan, J. Appell, P. Bassereau, G. Porte, and R. May, J. Phys. (France) **50**, 2553 (1989).
[30] J. Appell and J. Marignan, J. Phys. II **1**, 1447 (1991).
[31] M.E. Cates and S.J. Candau, J. Phys.: Condens. Matter **2**, 6869 (1990).
[32] G. Massiera, Thesis, Université de Montpellier II (2002).
[33] J.S. Pedersen and P. Schurtenberger, Europhys. Lett. **45**, 666 (1999).
[34] Equation (7) does not take into account an instrumental function (IF). By convoluting the theoretical structure factor with an IF, we have, however, checked that the instrumental resolution does not lead to any significant shift of the peak position.